

Thyroid hormone receptor regulates most genes independently of fibroblast growth factor 21 in liver

Aijun Zhang¹, Douglas H Sieglaff¹, Jean Philippe York¹, Ji Ho Suh¹, Stephen D Ayers^{1,*}, Glenn E Winnier¹, Alexei Kharitonov², Christopher Pin^{3,4}, Pumin Zhang⁵, Paul Webb¹ and Xuefeng Xia^{1,6}

¹Houston Methodist Research Institute, Genomic Medicine Program, 6670 Bertner Ave, Houston, Texas 77030, USA

²College of Arts and Sciences, Chemistry Department, Indiana University Bloomington, Bloomington, Indiana, USA,

³Departments of Paediatrics, Oncology, and Physiology and Pharmacology, University of Western Ontario, London, Ontario, Canada

⁴Children's Health Research Institute, London, Ontario, Canada

⁵Department of Molecular Physiology and Biophysics, Baylor College of Medicine, Houston, Texas, USA

⁶The Third Affiliated Hospital of Guangzhou Medical University, Guangzhou, China

*S D Ayers is now at Personalis Inc., Department of Genomics, Menlo Park, CA, USA

Correspondence should be addressed to X Xia or P Webb

Emails
xxia2@tmhs.org or pwebb@tmhs.org

Abstract

Thyroid hormone (TH) acts through specific receptors (TRs), which are conditional transcription factors, to induce fibroblast growth factor 21 (FGF21), a peptide hormone that is usually induced by fasting and that influences lipid and carbohydrate metabolism via local hepatic and systemic endocrine effects. While TH and FGF21 display overlapping actions when administered, including reductions in serum lipids, according to the current models these hormones act independently *in vivo*. In this study, we examined mechanisms of regulation of FGF21 expression by TH and tested the possibility that FGF21 is required for induction of hepatic TH-responsive genes. We confirm that active TH (triiodothyronine (T₃)) and the TR β -selective thyromimetic GC1 increase FGF21 transcript and peptide levels in mouse liver and that this effect requires TR β . T₃ also induces FGF21 in cultured hepatocytes and this effect involves direct actions of TR β 1, which binds a TRE within intron 2 of FGF21. Gene expression profiles of WT and *Fgf21*-knockout mice are very similar, indicating that FGF21 is dispensable for the majority of hepatic T₃ gene responses. A small subset of genes displays diminished T₃ response in the absence of FGF21. However, most of these are not obviously directly involved in T₃-dependent hepatic metabolic processes. Consistent with these results, T₃-dependent effects on serum cholesterol are maintained in the *Fgf21*^{-/-} background and we observe no effect of the *Fgf21*-knockout background on serum triglycerides and glucose. Our findings indicate that T₃ regulates the genes involved in classical hepatic metabolic responses independently of FGF21.

Key Words

- ▶ nuclear receptor
- ▶ FGF
- ▶ gene expression
- ▶ metabolism

Journal of Endocrinology
(2015) 224, 289–301

Introduction

Fibroblast growth factor 21 (FGF21) is one of three endocrine FGFs that influence metabolic responses via a combination of local and systemic actions. FGF21 is

expressed in the liver, pancreas, and white and brown adipose tissue (Johnson *et al.* 2009, Fon Tacer *et al.* 2010, Klierer & Mangelsdorf 2010). Hepatic *Fgf21* expression is

induced by the nuclear hormone receptor peroxisome proliferator-activated receptor α (PPAR α) under fasting conditions, and secreted FGF21 peptide exerts autocrine/paracrine effects on liver, including regulation of genes involved in lipogenesis, lipolysis, and fatty acid oxidation, as well as additional endocrine effects on other tissues (Badman *et al.* 2007). Administration of FGF21 to overweight and diabetic mice results in decreases in the levels of plasma triglycerides and glucose, and increases in both insulin sensitivity and thermogenesis associated with decreased body weight (Coskun *et al.* 2008, Berglund *et al.* 2009, Xu *et al.* 2009). Conversely, mice that lack FGF21 exhibit late-onset obesity. Thus, there is intense interest in FGF21 as a therapeutic for metabolic disorders, weight loss, and diabetes. Potentially adverse effects of FGF21 have also come to light. FGF21 is involved in integration of metabolism and bone turnover, raising the possibility that FGF21 could promote bone loss, and elevated FGF21 levels are associated with abnormal lipid profiles in coronary heart disease, raising concerns about cardiovascular events (Iglesias *et al.* 2012, Wei *et al.* 2012). Moreover, FGF21 levels become elevated in obesity and nonalcoholic fatty liver disease, indicating that serum FGF21 levels do not always correlate with an improved metabolic profile. Given these concerns, it is important to understand how to manage local production of FGF21 in desired target tissues and the consequences of changes in FGF21 concentrations.

Thyroid hormones (THs) act as master regulators of metabolism and there is evidence for interdependency of TH and FGF21 signaling pathways. TH receptors (TR α and TR β) are members of the nuclear hormone receptor family that regulate target genes in response to the main active form of TH, triiodothyronine (T₃). TRs usually work by binding DNA-response elements (TREs) in the proximal promoters of target genes as heterodimers with retinoid X receptors (RXRs) but can also regulate target genes via protein–protein interactions with heterologous transcription factors (Baxter & Webb 2009, Cheng *et al.* 2010, Lin *et al.* 2013). T₃ induces FGF21 in mouse liver and, in this study, TR β selectively enhances FGF21 expression and promoter activity via interactions with PPAR α bound to PPAR α -response elements, but does not require PPAR α to induce other T₃-regulated genes (Adams *et al.* 2010). In addition, FGF21 administration to mice reduces serum levels of the parental form of TH, thyroxine (T₄), and T₃, implying mutual regulatory dependency of these signaling systems (Domouzoglou *et al.* 2014). In spite of these potential relationships, key actions of FGF21 and TH appear largely independent (Domouzoglou *et al.* 2014). Recent assessments of administration of TH to *Fgf21*-knockout mice have revealed no differences in serum lipids,

the expression of selected T₃-regulated genes in liver and brown adipose tissue, or overall energy expenditure. Conversely, FGF21 elicited similar alterations in serum lipids and gene expression in hypothyroid and euthyroid mice.

In this study, we set out to understand the mechanisms and downstream effects of TH-dependent changes in hepatic *Fgf21* expression. We find that both T₃ and the TR β -selective thyromimetic GC1 act through TR β to directly induce FGF21 expression and that the *Fgf21* locus harbors a functional TRE within intron 2. This finding added another layer of complexity to previous studies of T₃ regulation of FGF21 expression, which indicated that TR β works primarily through PPAR α bound to the *FGF21* promoter (Adams *et al.* 2010). While patterns of hepatic T₃ responses are similar in WT and *Fgf21*-knockout mice, similar to previous studies of a subset of hepatic genes involved in lipid metabolism (Domouzoglou & Maratos-Flier 2011, Domouzoglou *et al.* 2014), we also find that optimal response of a small subset of hepatic TH-target genes requires *Fgf21*. These genes, however, are not obviously related to metabolic regulation and we find no changes in serum metabolic parameters in *Fgf21*-knockout mice. Thus, our data support the idea that hepatic effects of TH on gene regulation and metabolism are largely independent of *Fgf21*.

Materials and method

Mice

All animal experiments were approved by the Animal Care and Use Committee of Houston Methodist Hospital Research Institute. Mouse strains C57BL/6, *ApoE*^{-/-}, *Ldlr*^{-/-}, and *TRβ*^{-/-} were purchased from The Jackson Laboratory (Bar Harbor, ME, USA) at 9 weeks of age. *Fgf21*^{-/-} mice on a C57/BL6 background (Dutchak *et al.* 2012) were received from The University of Texas Southwestern Medical Center (Dallas, TX, USA). For short-term ligand treatments (1 and 3 days) T₃, GC1, or vehicle (control) were administered to mice ($n=5$) by oral gavage at a dose of 1 mg/kg body weight, after which, mice were killed and dissected for tissue harvesting. For long-term treatments (2 weeks), GC1 was admixed into diet at a dose of 0.8 mg/kg body weight, after which the mice were killed for collection of blood and tissue samples.

Quantitative RT-PCR

Total RNA was isolated from livers or cultured cells using the RNAeasy Kit (Qiagen) and reverse transcribed to cDNA using the ABI Reverse Transcription Kit according to the

manufacturer's instructions. Gene transcript expression was measured by quantitative RT-PCR (qPCR) (Roche LightCycler 480 II), in 20 µl reactions that included cDNA (10 ng of initial RNA input), 900 nM of each primer, PCR-grade water, and 10 µl of 2× TaqMan Master Mix (Applied Biosystems). The transcript expression levels were normalized to peptidylprolyl isomerase A (PPIA) expression levels. Independent samples were prepared from five to six different mice per genotype or three separate cell culture seedings and analyzed in technical triplicates. Gene transcript abundance was assessed by the standard $\Delta\Delta C_p$ method and results were expressed as relative fold change compared with respective control group. Primer catalog numbers are available on request.

Serum FGF21 analyses

Mouse serum FGF21 concentrations were determined by ELISA (Phoenix Secretomics (Burlingame, CA, USA), PS001-01-EK-M-1), according to the manufacturer's protocol. Serum samples of six to seven mice from each treatment were analyzed.

Immunoblot analysis

One hundred micrograms of liver were homogenized in 1 ml homogenization buffer (10 mM Tris-HCl (pH 7.5), 5 mM EDTA, 150 mM NaCl, 30 mM sodium phosphate, 10% glycerol, 0.5% NP40) containing complete protease inhibitor cocktail (Roche) using a Polytron homogenizer. The homogenate was centrifuged at 14 000 g for 8 min at 4 °C and the supernatant collected for further analysis. The proteins were separated by SDS-PAGE, transferred to polyvinylidene difluoride membranes (Millipore, Billerica, MA, USA), and detected with primary FGF21 and β -actin (Sigma) antibodies at 1:1000 and 1:10 000 dilutions, respectively, and HRP-conjugated secondary antibody at 1:5000 dilution. Immunoreactive proteins were visualized using the ECL western blotting detection system (Amersham, RPN2106), and densitometry analysis was conducted with Scion Image v4.0.3.2 software.

Cell culture

HepG2 (ATCC, Bethesda, MD, USA) and HepG2-TR β (Lin *et al.* 2013) cells were grown in DMEM supplemented with 10% fetal bovine serum (FBS), 100 U/ml of penicillin, 0.1 g/l of streptomycin, and 4 mmol/l glutamine, under 95% air and 5% CO₂ at 37 °C. For cycloheximide (CHX) treatment, HepG2-TR β cells were maintained within 10% resin-stripped

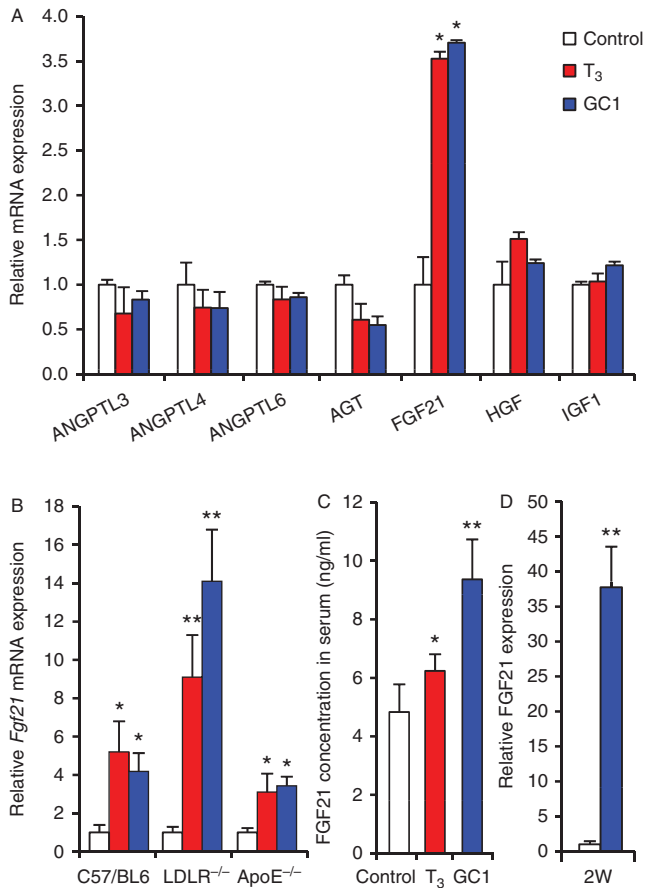
FBS-DMEM media for 24 h before treatment. The cells were pretreated with CHX at 10 µg/ml for 30 min, followed by 10 nM T₃ incubation for 6 h, after which RNA was collected using the RNAeasy Kit (Qiagen). For RNA interference assays, HepG2-TR β cells were plated in 10% resin-stripped FBS-DMEM media and grown to 50% confluency. The cells were transfected with PPAR α ON-TARGET plus SMART pool or negative control siRNA (Dharmacon, Waltham, MA, USA) at a 50 nM final concentration, and 48 h later treated with 10 nM T₃ or bezofibrate for 6 h, after which RNA was collected using the RNAeasy Kit (Qiagen).

Chromatin immunoprecipitation

Chromatin immunoprecipitation (ChIP) was performed using the EZ ChIP Kits (Millipore) according to the manufacturer's instructions. Briefly, mice livers were homogenized with a hand-held homogenizer in PBS containing a broad-spectrum protease inhibitor cocktail and then cross-linked with 1% formaldehyde. The nuclei were collected by adding lysis buffer following cross-linkage, which was stopped through addition of glycine. The liver nuclear solution was sonicated with a Fisher 60 Sonic Dismembrator (Thermo Fisher Scientific, Waltham, MA, USA). The sonicated solution was incubated with anti-TR β polyclonal antibody or control rabbit IgG (Millipore) overnight with agitation at 4 °C. The TR β antibody used for ChIP has also been used for TR β ChIP studies of mouse cerebellum and liver (Dong *et al.* 2009, Paquette *et al.* 2011) and was originally purchased from Affinity Bioreagents (Golden, CO, USA), but was later made available through Thermo Fisher Scientific and Pierce (Grand Island, NY, USA), as PA1-213A. We have used the same antibody for western blotting analysis of TR β expression in cell lines and mouse liver with appropriate controls for TR β specificity shown (Ayers *et al.* 2014, Lammel Lindemann *et al.* 2014). Antibody-bound chromatin was precipitated with protein G-conjugated agarose beads, washed with gradient stringent buffers, and eluted with the elution buffer provided with the kit. The isolated DNA was analyzed by qPCR analysis using oligonucleotides corresponding to the following regions of the FGF21 locus: *Fgf21* +715/+902, forward: 5'-CAGACTGGCCCTCAGAGAAG-3', reverse: 5'-CTCTGCCTAGGTTGGCATTG-3'. *Fgf21* +3727/+3880 forward: 5'-CATGTGGATTCTGGGATTG-3', reverse: 5'-GACCAGGCTGGACTCAAGTT-3'.

Transient transfection

For cloning of *Fgf21-luciferase* reporters, a 339-bp fragment of *Fgf21* intron 2 was PCR amplified from C57BL/6 mouse

**Figure 1**

Fgf21 is upregulated in livers of T₃-treated mice. (A) Results of qRT-PCR analysis of hepatic FGF21 transcript levels in WT (C57BL/6) mice treated with T₃ or GC1 for 24 h ($n=6$ /group) along with other secreted hepatic factors, as follows: angiopoietin-like factors (ANGPTL) 3, 4, and 6; angiotensinogen (AGT), hepatocyte growth factor (HGF), insulin-like growth factor 1 (IGF1). (B) Hepatic *Fgf21* mRNA levels in LDL receptor knockout (*Ldlr*^{-/-}) and apolipoprotein E-knockout (*ApoE*^{-/-}) mice treated with T₃ or GC1 for 24 h ($n=6$ /group). (C) Circulating levels of FGF21 in *Ldlr*^{-/-} mice treated with T₃ or GC1 for 24 h ($n=6$ /group). (D) Hepatic *Fgf21* mRNA levels in *Ldlr*^{-/-} mice 28 days following GC1 treatment ($n=6$ /group). Statistical significance of the observed changes is denoted by single or double asterisks, which indicate and refers to $P<0.05$ or $P<0.01$ respectively.

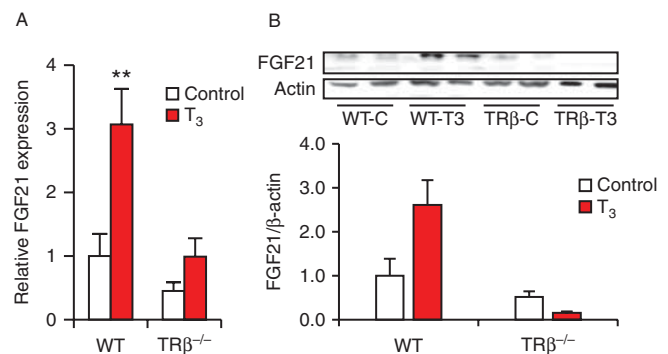
gDNA and cloned into the BglII and HindIII sites of pGL4-23. Positive clones were confirmed through sequencing. For luciferase assays, HepG2-TRβ1 cells (2×10^5 cells/well) were seeded into six-well plates 12 h before transfection of 1 μg/well of *Fgf21-luciferase* reporter constructs and 0.1 μg/well of *Renilla-luciferase* control plasmid using Fugene 6 transfection reagent. Twenty-four hours post transfection, cells were incubated with 10 nM T₃ for another 24 h, after which luciferase activity was determined using the Promega Dual Luciferase Assay Kit following the manufacturer's instructions.

Electrophoretic mobility shift assay

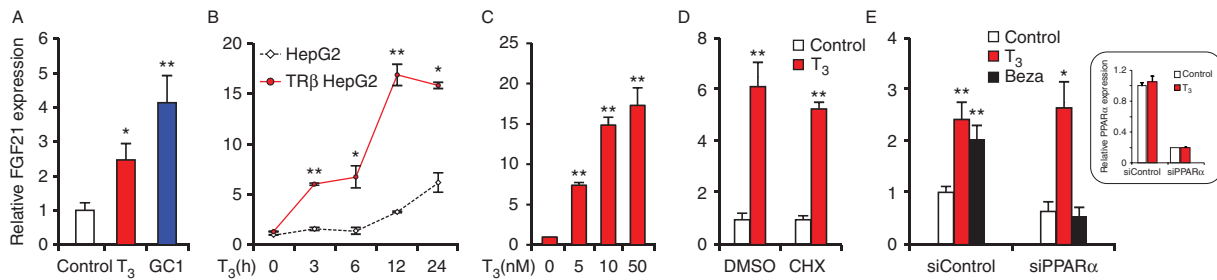
Electrophoretic mobility shift assay (EMSA) was performed by incubating ³²P-labeled oligonucleotide probes with *in vitro* translated TRβ and RXRα. The results were visualized by autoradiography. Competition assays were performed by adding 100× molar excess of either unlabeled oligonucleotide probes (specific competitor) or unlabeled mutant oligonucleotide probe (nonspecific competitor, mutated bases are indicated in each figure).

Microarray analysis

Mouse WG-6 v2 whole-genome expression arrays were purchased from Illumina (San Diego, CA, USA), and cRNA synthesis and labeling were performed using Illumina TotalPrep-96 RNA Amplification Kit (Ambion, Austin, TX, USA), with the labeling *in vitro* transcription reaction performed at 37 °C for 14 h. Biotinylated cRNA samples were hybridized to arrays at 58 °C for 18 h according to the manufacturer's protocol. Arrays were scanned using BeadArray Reader (Illumina). Unmodified microarray data obtained from GenomeStudio were background-subtracted and quantile-normalized using the lumi package (Du *et al.* 2008) and analyzed with the limma package (Smyth 2005) within R (R Development Core Team 2010). All analysis was corrected for multiple hypotheses testing (Benjamini & Hochberg 1995) and effects were determined to be significant when there was a greater than or equal to twofold increase/decrease relative to the control and they had an adjusted P value <0.05 . Raw microarray data sets have been deposited in the NCBI Gene Expression Omnibus (GEO)

**Figure 2**

Fgf21 induction requires TRβ. (A) qRT-PCR analysis of hepatic *Fgf21* transcript levels in WT (C57BL/6) mice treated with T₃ for 24 h or *Trβ*^{-/-} knockout mice ($n=6$ /group). (B) Western blotting analysis of hepatic FGF21 protein levels in WT and *Trβ*^{-/-} mice with representative gel images at the top and quantitation below. The statistical significance of the observed changes is denoted by double asterisks, which indicate $P<0.01$.

**Figure 3**

TR β -dependent induction of FGF21 in cultured cells. (A) FGF21 mRNA levels in HepG2 cells treated with GC1 (10 nM), T $_3$ (10 nM) or vehicle for 24 h ($n=4$). (B) Expression levels of FGF21 mRNA in HepG2 cells that express exogenous TR β or in parental HepG2 cells examined by RT-qPCR at different time points after T $_3$ induction ($n=4$). (C) T $_3$ concentration dependence of induction of FGF21 mRNA in HepG2 cells that expressed exogenous TR β was examined by RT-qPCR for various concentrations of T $_3$ for 24 h ($n=4$). (D) T $_3$ induction of FGF21 mRNA is insensitive to CHX. Cells

were pretreated with CHX for 30 min, followed by T $_3$ for 6 h. (E) PPAR α knockdown does not affect T $_3$ response of FGF21 in HepG2 cells. qRT-PCR analysis of FGF21 transcript levels after treatment of HepG2-TR β cells with bezofibrate or T $_3$ for 2 h. Results are shown in the presence of control scrambled siRNA or PPAR α -specific siRNA. Knockdown levels of PPAR α transcripts are shown in the inset. The statistical significance of the observed changes is denoted by single or double asterisks, which indicate $P<0.05$ and $P<0.01$ respectively.

database under accession number GSE58062. Microarray data was also validated through qPCR (TaqMan) analysis, showing excellent correlation $R^2=0.85$ ($n=59$).

Data analysis and statistics

All values are expressed as mean \pm s.e.m. Statistical analyses were performed using GraphPad Prism Version 5.0 Software (GraphPad, Inc., San Diego, CA, USA). Data were analyzed by Student's t -test, Mann-Whitney U test, or one-way ANOVA, where P values <0.05 were considered to be statistically significant.

Serum metabolites

Serum aliquots were sent to the comparative pathology laboratory of Baylor College of Medicine (Houston, TX, USA) for serum chemistry analysis.

Results

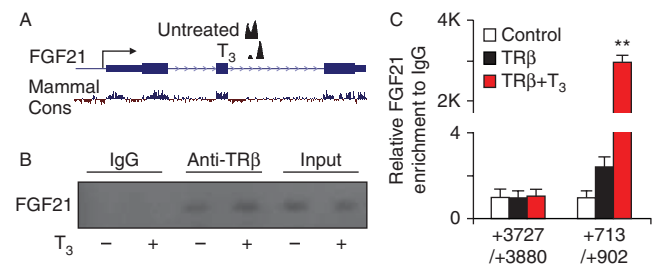
T $_3$ and GC1 induce *Fgf21* in liver in a TR β -dependent manner

We examined the effects of acute (24 h) treatment of male C57BL/6 mice with T $_3$ or the thyromimetic GC1 on hepatic *Fgf21* expression. *Fgf21* mRNA was induced by both ligands, an effect not observed for genes that encode other secreted hepatic factors (Fig. 1A). Similar effects of TR ligands on *Fgf21* expression were seen in two mouse models of dyslipidemia (*ApoE*^{-/-} and *Ldlr*^{-/-}) (Fig. 1B) and FGF21 induction was accompanied by increases in circulating FGF21 peptide in serum (Fig. 1C). The selective

thyromimetic GC1 also elicited increases in hepatic *Fgf21* expression, which persisted for at least 2 weeks with continuous treatment (Fig. 1D). Optimal hepatic T $_3$ induction of FGF21 required TR β , the predominant TR subtype in liver (Fig. 2A and B). Thus, T $_3$ acts primarily through TR β to induce hepatic *Fgf21* expression.

TR β directly induces *Fgf21* in cultured cells

To define the mechanisms of TH-dependent induction of hepatic *Fgf21* expression, we examined the response of *Fgf21* mRNA to T $_3$ or GC1 in human HepG2 cells that stably express TR β (Lin *et al.* 2013). We observed induction of FGF21 following short-term treatment with either ligand (Fig. 3A). This effect persisted over several time points (Fig. 3B and

**Figure 4**

A TR β -binding site in the FGF21 second intron. (A) Results of ChIP-Seq analysis with HepG2-TR β cells showing binding events in the FGF21 second intron. (B) Representative gel showing results of ChIP analysis with an anti-TR β 1 antibody to verify binding within FGF21 intron 2 along with an IgG control. (C) qRT-PCR analysis of ChIP experiments showing specific binding of TR β 1 to the FGF21 intron 2 in native mouse liver. Immunoprecipitations were carried out with either TR β antibodies or control IgG, and immunopurified DNA was analyzed with primers flanking intron 2 of FGF21 (+715 to 902) or a control region (+3727 to +3880) ($n=4$). The statistical significance of the observed changes is denoted by double asterisks, which indicate $P<0.01$.

results not shown). A modest T_3 response was also observed in parental HepG2 cells after extended T_3 treatment (Fig. 3B); this delayed effect resembles the kinetics of T_3 induction of other bona fide hepatic TR-target genes in this cell type and is probably a consequence of low levels of TR β that are present in these cells (Yuan *et al.* 2012). T_3 -dependent FGF21 induction exhibited classical dose dependence with maximal activation with 10 nM hormone (Fig. 3C), implying that this T_3 effect was TR-dependent, and was maintained after pretreatment with the protein synthesis inhibitor CHX, implying a direct transcriptional effect of TR (Fig. 3D). Interestingly, the effects of TR β on FGF21 expression were

not absolutely dependent on PPAR α in HepG2 (Fig. 3E). Although induction of *Fgf21* mRNA by the PPAR α ligand bezofibrate was abrogated by a PPAR α -specific siRNA that reduced PPAR α transcript levels by 80% (inset), the T_3 response was unaffected.

A functional TRE in the *Fgf21* second intron

To determine whether TR β might bind the *Fgf21* locus independently of PPAR α , we consulted a published ChIP-chip dataset and our own preliminary ChIP-Seq results. Results of recent studies have indicated the

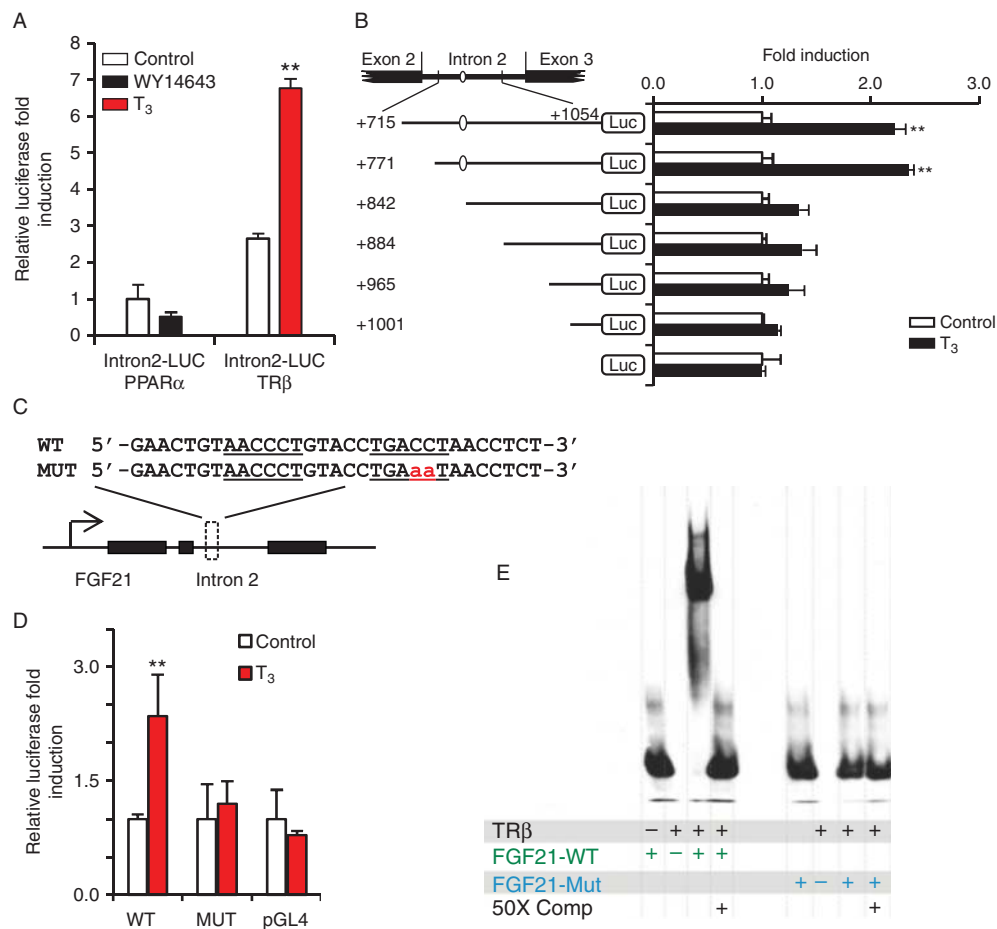


Figure 5

An intronic TRE in the *FGF21* locus. (A) Reporter assays were performed in HepG2-TR β 1 cells co-transfected with a reporter construct harboring intron 2 of *FGF21* in the presence of PPAR α or TR β expression plasmid. The cells were treated with either 100 nM WY14643 or 10 nM T_3 ($n=4$). (B) As shown in Fig. 5A, results of luciferase assays performed with a variety of reporter genes bearing intron 2 truncations are shown in the schematic diagram. (C) Diagrammatic representation of the *FGF21* promoter within the reporter vector (the region that displayed enrichment within the ChIP-assay). The *FGF21* promoter used in our studies contains binding sites for TR β . The TRE determined to mediate the TR β -response is also shown, as indicated by truncation and mutant analysis. (D) As shown in Fig. 5A, HepG2-TR β 1 cells

co-transfected with a reporter construct harboring intron 2 of *FGF21* or TRE-mutant reporter constructs or control vector pGL4 in the presence of TR β expression plasmid. The cells were treated with either vehicle or 10 nM T_3 ($n=4$). (E) Electrophoretic mobility shift assay (EMSA) depicting TR β binding to the discovered TRE. The response elements were measured by mixing 100 ng of purified TR β (DBD-LBD) with 1 pM of biotin-labeled double-stranded oligonucleotide corresponding to +715 to +1054 of *FGF21*. Binding specificity of the regulatory region was verified with competition experiments in which 50-fold molar excess of unlabeled +715/+1054 oligomer or mutant-TRE +715/+1054 oligomer ($n=4$). The statistical significance of the observed changes is denoted by double asterisks, which indicate $P<0.01$.

presence of an intronic TR β -binding peak within the *Fgf21* locus in mouse cerebellum (Dong *et al.* 2009) and we later confirmed the existence of this peak in the data derived from our own ChIP-Seq analysis of TR β -binding events in HepG2 cells (Fig. 4A) (Ayers *et al.* 2014). We verified TR β binding at this location with conventional ChIP-PCR performed on human HepG2-TR β cells (Fig. 4B) and on native mouse liver (Fig. 4C).

Cloned sequences corresponding to the second intron of human *FGF21* conferred T₃ responsiveness upon a luciferase reporter (Fig. 5A). There was no response to PPAR α ligand (WY14643). Deletion mapping indicated that important T₃-responsive elements lay between the intronic sequences +771 and +842 downstream of the *Fgf21* transcriptional start site (Fig. 5B). This region of the mouse gene harbored a degenerate nonconsensus TRE (DR-5) with one well conserved half site (AGGTCA; reverse strand TCCAGT) (Fig. 5C). Mutation of the putative TRE blocked the responses to T₃ of the *Fgf21*-dependent luciferase reporter (Fig. 5D). Furthermore, the putative TRE bound bacterially expressed TR β in EMSA and this interaction was abolished by mutation of the AGGTCA sequence or an excess of WT oligonucleotide (Fig. 5E).

Altered hepatic T₃-responses in *Fgf21*^{-/-} mice

As T₃ induces FGF21 in liver, and secreted FGF21 peptide may exert autocrine/paracrine effects upon gene expression in hepatocytes, we determined whether T₃ regulated the same genes in the livers of WT and euthyroid *Fgf21*^{-/-} mice using Illumina BeadArray analysis. More than 500 gene transcripts displayed significant response (greater than or equal to twofold with an adjusted *P* value <0.05) to a 3-day T₃ treatment in WT mice, in accordance with previous studies. In general, T₃-dependent gene regulation patterns were similar in both WT and *Fgf21*-knockout mice and the majority of T₃ responses differed by not more than 50% (black points located within the dotted lines that delimit a twofold difference between WT and *Fgf21*^{-/-} mice) (Fig. 6A).

We detected two clusters of genes with altered T₃ response in the *Fgf21*^{-/-} background (red points, outside of dotted delimiting lines). One group (Table 1, 31 genes) exhibited diminished T₃-dependent activation in the *Fgf21*^{-/-} background, and the other altered group (Table 2, 23 genes) displayed diminished T₃-dependent repression. These altered responses to T₃ were readily reproduced in independent high-throughput qRT-PCR experiments (Fig. 6B). Examples of such genes with diminished responses to T₃ in the *Fgf21*-knockout mice include *Dio1*, *Insig2*, *Cdkn1*, and *Glut1* (Fig. 6C, full gene

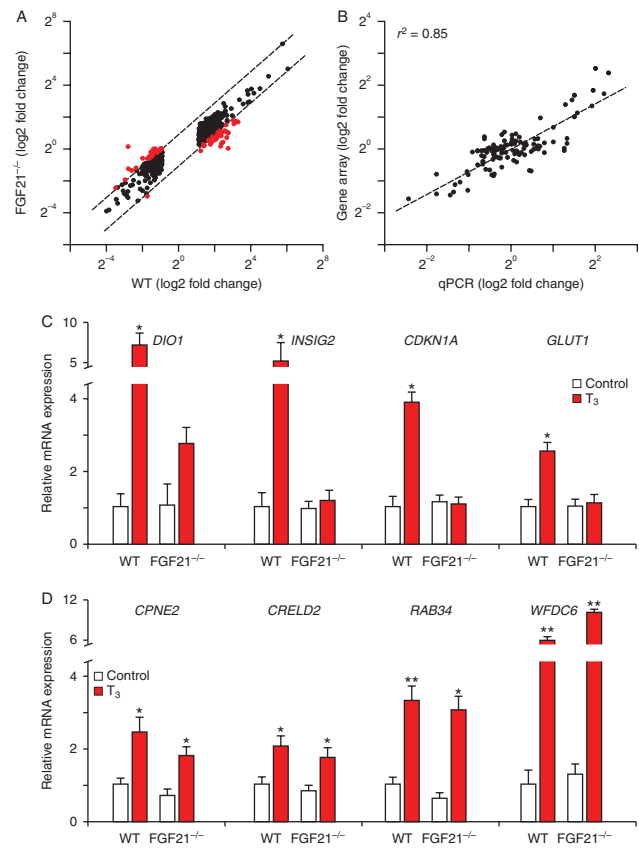


Figure 6

Similar patterns of T₃ responses in WT and *Fgf21*-knockout mice. (A) Scatter plots of T₃ responses in livers of WT and *Fgf21*-knockout mice treated with T₃ for 3 days. Dots represent genes that were induced or repressed at least twofold by T₃ treatment with an adjusted *P* value of <0.05. Dotted lines represent a twofold deviation from WT values. (B) qPCR validation of the microarray data. *R*² = 0.85 (*n* = 59). (C) Representative qPCR verification of genes that display diminished responses to T₃ in the *Fgf21*^{-/-} background. (D) Representative qPCR verification of genes that display unchanged responses to T₃ in the *Fgf21*^{-/-} background. The statistical significance of the observed changes is denoted by single or double asterisks, which indicate *P* < 0.05 and *P* < 0.01 respectively.

names in Table 1). Genes that displayed similar levels of T₃ response in both strains include *Cpne2*, *Rab34*, *Creld2*, and *Wfdc6*, as identified in our previous studies (Lin *et al.* 2013) (Fig. 6D). Thus, targeted ablation of *Fgf21* in the mouse germ line did not result in the global inhibition of a large percentage of hepatic T₃ responses, but FGF21 was required for induction of a small subset of T₃-regulated genes.

We could not perceive many obvious relationships between genes that display altered responses to T₃ in the *Fgf21*-knockout mice and canonical hepatic metabolic process regulated by TH (Tables 1, 2, and 3). Results of ingenuity pathway analysis (IPA) indicated that the gene subsets that showed altered T₃ response in the *Fgf21*-knockout background might affect the action of vitamin C,

Table 1 Positively T₃-regulated genes influenced by *Fgf21* knockout

Probe_ID	Symbol	Entrez gene name	Fold change		Adjusted P value	
			WT	<i>Fgf21</i> KO	WT	<i>Fgf21</i> KO
ILMN_2874352	<i>Cyp17A1</i>	Cytochrome P450, family 17, subfamily A	8.861	3.110	0.000	0.029
ILMN_2647234	<i>Dio1</i>	Deiodinase, iodothyronine, type I	8.268	3.229	0.023	0.227
ILMN_2813830	<i>Nt5e</i>	5'-nucleotidase, ecto (CD73)	7.634	2.870	0.001	0.060
ILMN_3009501	<i>Kcnk1</i>	Potassium channel, subfamily K, member 1	7.393	3.370	0.003	0.050
ILMN_1241350	<i>Vsig4</i>	V-set and immunoglobulin domain containing 4	6.151	1.941	0.016	0.420
ILMN_1239959	<i>E030018b13rik</i>	RIKEN cDNA E030018B13 gene	6.088	-1.005	0.020	0.998
ILMN_2619620	<i>C1qb</i>	Complement component 1, q subcomponent, B chain	6.041	1.988	0.010	0.343
ILMN_2715840	<i>C1qc</i>	Complement component 1, q subcomponent, C chain	5.785	1.596	0.009	0.540
ILMN_2775030	<i>Folr2</i>	Folate receptor 2 (fetal)	5.643	2.751	0.002	0.039
ILMN_2528155	<i>Loc227995</i>	Predicted gene 13607, actin-like 6A pseudogene	5.618	2.070	0.021	0.368
ILMN_2878071	<i>Lyz1/Lyz2</i>	Lysozyme 2	5.506	2.081	0.009	0.265
ILMN_1234858	<i>Insig2</i>	Insulin-induced gene 2	5.022	1.302	0.035	0.830
ILMN_2671923	<i>Ly86</i>	Lymphocyte antigen 86	4.760	1.954	0.004	0.185
ILMN_1252636	<i>Mmd2</i>	Monocyte to macrophage differentiation-associated 2	4.749	1.231	0.011	0.824
ILMN_2925653	<i>Ear2</i>	Eosinophil-associated, ribonuclease A family, # 2	4.691	1.715	0.025	0.499
ILMN_2634083	<i>Cdkn1a</i>	Cyclin-dependent kinase inhibitor 1A (p21, CIP1)	4.595	1.083	0.013	0.947
ILMN_1216880	<i>Emr1</i>	EGF-like module containing, mucin-like, hormone receptor-like 1	4.462	1.711	0.022	0.466
ILMN_2640346	<i>P2ry13</i>	Purinergic receptor P2Y, G-protein-coupled, 13	4.249	2.000	0.005	0.158
ILMN_2785648	<i>Cd207</i>	CD207 molecule, langerin	4.242	1.781	0.006	0.260
ILMN_2533376	<i>Mmp27</i>	Matrix metalloproteinase 27	4.132	1.960	0.025	0.319
ILMN_2752524	<i>Paqr9</i>	Progesterin and adipoQ receptor family member IX	3.988	1.724	0.045	0.505
ILMN_2524986	<i>Ear3</i>	Eosinophil-associated, ribonuclease A family, #3	3.869	1.493	0.028	0.599
ILMN_2948296	<i>Wfdc12</i>	WAP four-disulfide core domain 12	3.706	1.438	0.020	0.601
ILMN_2819319	<i>Rrm2</i>	Ribonucleotide reductase M2	3.687	1.627	0.000	0.100
ILMN_1241695	<i>Ms4a6a</i>	Membrane-spanning 4-domains, subfamily A, member 6A	3.376	1.641	0.020	0.380
ILMN_2896170	<i>Apcs</i>	Amyloid P component, serum	3.291	1.301	0.043	0.761
ILMN_3118707	<i>Sla</i>	Src-like-adaptor	3.113	1.191	0.023	0.824
ILMN_2548010	<i>Hopx</i>	HOP homeobox	2.970	1.422	0.016	0.491
ILMN_2788073	<i>Hmox1</i>	Heme oxygenase (decycling) 1	2.882	1.411	0.005	0.357
ILMN_2761585	<i>2400009b08RIK</i>	RIKEN cDNA 2400009B08 gene	2.409	1.109	0.020	0.870
ILMN_2728300	<i>Mdm1</i>	<i>Mdm1</i> nuclear protein homolog (mice)	2.386	1.185	0.003	0.597
ILMN_1258159	<i>Glut1</i>	Glucose transporter 1	1.580	1.087	0.041	0.870

the complement pathway, and other processes (Table 3 and results not shown). Similar biological functions were predicted through Genecodis analysis (Tabas-Madrid *et al.* 2012) (not shown). More directed queries in which we utilized IPA function pathway analysis to probe for the association of defined hepatic metabolic pathways with the T₃/FGF21-dependent gene subset revealed the connections of several members of this gene set with different aspects of lipid metabolism, amino acid metabolism, and carbohydrate metabolism (Table 4). Inspection of these relationships did not allow us to generate many obvious predictions about the

influences of these genes upon local hepatic and systemic metabolism (see 'Discussion').

Given that there were weak associations of the T₃/FGF21-dependent gene set with classical T₃-dependent hepatic metabolic pathways, we determined whether *Fgf21*-knockout influenced the levels of serum metabolites under the conditions of our experiment (Fig. 7). Previously, treatment with T₃ and a thyromimetic has been shown to result in rapid reductions in serum cholesterol levels in WT mice (Lin *et al.* 2012, Lammel Lindemann *et al.* 2014). While we were able to reproduce this effect with short T₃

Table 2 Negatively T₃-regulated genes influenced by *Fgf21* knockout

Probe_ID	Symbol	Entrez gene name	Fold change		Adjusted P value	
			WT	<i>Fgf21</i> KO	WT	<i>Fgf21</i> KO
ILMN_2852624	<i>Hamp/Hamp2</i>	Hepcidin antimicrobial peptide	-11.73	-5.569	0.006	0.049
ILMN_1253233	<i>Dsg1c</i>	Desmoglein 1 gamma	-8.159	-3.932	0.002	0.029
ILMN_2976211	<i>Cyp2b23</i>	Cytochrome P450, family 2, subfamily b, polypeptide 23	-7.294	1.075	0.022	0.970
ILMN_2796472	<i>Vldlr</i>	Very-LDL receptor	-7.191	-2.436	0.011	0.253
ILMN_1232758	<i>Gm3065</i>	Predicted gene 3065	-4.219	-1.550	0.010	0.480
ILMN_1214219	<i>Col27a1</i>	Collagen, type XXVII, alpha 1	-3.491	-1.564	0.001	0.189
ILMN_1230145	<i>Acvr2b</i>	Activin A receptor, type IIB	-3.352	-1.575	0.032	0.488
ILMN_2565942	<i>Flnb</i>	Filamin B, beta	-3.277	-1.451	0.038	0.605
ILMN_1256423	<i>Ranbp3l</i>	RAN-binding protein 3-like	-3.274	-1.440	0.009	0.452
ILMN_1218441	<i>Slc23a3</i>	Solute carrier family 23, member 3	-3.073	-1.479	0.030	0.519
ILMN_2875737	<i>Cyp2d6</i>	Cytochrome P450, family 2, subfamily D, polypeptide 6	-2.945	-1.313	0.022	0.655
ILMN_2523012	<i>Meg3</i>	Maternally expressed 3	-2.936	-1.143	0.033	0.879
ILMN_2625233	<i>9130230I23rik</i>	RIKEN cDNA 9130230L23 gene	-2.890	-1.395	0.026	0.559
ILMN_1213804	<i>Lrp4</i>	LDL receptor-related protein 4	-2.767	-1.030	0.020	0.975
ILMN_2624328	<i>Adamts7</i>	ADAM metalloproteinase with thrombospondin type 1 motif, 7	-2.635	-1.154	0.002	0.713
ILMN_1239872	<i>5830473c10rik</i>	RIKEN cDNA 5830473C10 gene	-2.597	-1.026	0.011	0.975
ILMN_1227319	<i>Vwce</i>	Von Willebrand factor C and EGF domains	-2.440	-1.212	0.011	0.662
ILMN_1247135	<i>Znf276</i>	Zinc finger protein 276	-2.209	-1.095	0.007	0.838
ILMN_2764325	<i>Bricd5</i>	BRICHOS domain containing 5	-2.202	-1.089	0.036	0.902
ILMN_2587761	<i>Kif1b</i>	Kinesin family member 1B	-2.135	-1.021	0.033	0.980
ILMN_2954098	<i>Lgals6</i>	Lectin, galactose-binding, soluble 6	-2.065	-1.024	0.011	0.969
ILMN_2718600	<i>Nfyb</i>	Nuclear transcription factor Y, beta	-2.061	-1.027	0.005	0.956
ILMN_2622891	<i>C12orf43</i>	Chromosome 12 open reading frame 43	-2.059	-1.028	0.044	0.973

treatments (Fig. 7A), it was unaltered in the *Fgf21*-knockout background. No T₃- or *Fgf21*-dependent changes in serum triglyceride or glucose levels were detected during the course of this treatment (Fig. 7B and C).

Discussion

PPAR α -dependent induction of FGF21 is required for changes in expression of genes that are involved in the fasting response in liver, and secreted hepatic *Fgf21* influences local hepatocyte metabolism and communicates information from liver to other tissues to coordinate fasting responses. Thus, FGF21 has attracted attention as a possible therapeutic to modulate metabolic disease. In this study, we verified previous observations which indicate that T₃ induces hepatic FGF21 production (Adams *et al.* 2010, Domouzoglou *et al.* 2014), and further dissected the mechanism of this effect and tested the possibility that FGF21 is required for T₃-dependent changes in local hepatic T₃ responses. Our results therefore support the concept that T₃ and FGF21 signaling pathways exhibit mutual regulatory dependence, but function largely independently (Domouzoglou *et al.* 2014).

T₃ acts through TR β to directly induce FGF21 expression. We extended previous studies (Adams *et al.* 2010,

Domouzoglou *et al.* 2014) to show that sustained TR-dependent induction of FGF21 is elicited by a selective TR β modulator and is dependent on TR β . Furthermore, similar effects were also observed in a human liver cell line (HepG2), in which FGF21 induction was amplified in the presence of exogenous TR β 1, and T₃-dependent induction of FGF21 was also detectable in the presence of low endogenous levels of TR β 1 in this cell type (Yuan *et al.* 2012). Thus, the capacity for T₃ regulation of hepatic FGF21 production is conserved in humans and in cultured cells of hepatic origin. Finally, TR regulation of FGF21

Table 3 IPA canonical pathway analysis of T₃/FGF21-dependent genes

Ingenuity canonical pathways	-log (P value)	Ratio	Molecules
Antioxidant action of vitamin C	2.89	0.027	HMOX1, SLC23A3, PLA2G7
Complement system	2.61	0.057	C1QC, C1QB
Phospholipases	2.14	0.030	HMOX1, PLA2G7
Bladder cancer signaling	1.77	0.021	MMP27, CDKN1A
Pancreatic adenocarcinoma signaling	1.62	0.016	HMOX1, CDKN1A

Table 4 IPA function pathway analysis of metabolic pathway association with T₃/FGF21-dependent genes

Function and pathway	Number of molecules	P value	Molecules
Lipid Metabolism			
Concentration of cholesterol	4	0.0051	<i>Cdkn1a, Dio1, P2ry13, Vldlr</i>
Efflux of cholesterol	2	0.0192	<i>Apcs, Vldlr</i>
Accumulation of triacylglycerol	2	0.0139	<i>Insig2, Vldlr</i>
Conversion of lipid	3	0.0053	<i>Cyp17a1, Cyp2d6, Hmox1</i>
Quantity of steroid	5	0.0067	<i>Cdkn1a, Cyp17a1, Dio1, P2ry13, Vldlr</i>
Amino acid metabolism	2	0.0030	<i>Cdkn1a, Dio1</i>
Carbohydrate metabolism	3	0.0037	<i>Lyz1/Lyz2, Nt5e, Pla2g7</i>
Insulin-dependent diabetes mellitus	6	0.0012	<i>Col27a1, Ly86, Lyz1/Lyz2, Ms4a6a, Nt5e, P2ry13</i>

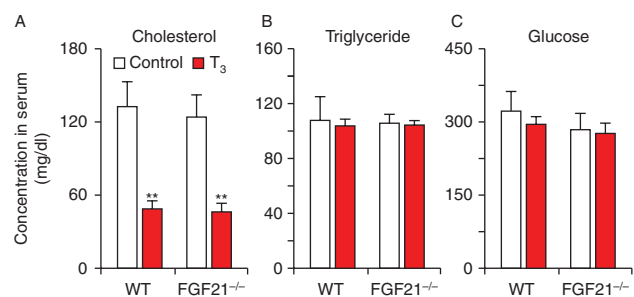
exhibits an appropriate T₃ dose response and is not affected by the protein synthesis inhibitor CHX, implying a direct effect of T₃ through TRs.

While TRs do not bind to the *Fgf21* proximal promoter, the results of studies by our own group and others indicate that TREs are often located within introns or the 3' downstream region of target genes (Chatonnet *et al.* 2013, Gagne *et al.* 2013, Ayers *et al.* 2014, Ramadoss *et al.* 2014). We therefore searched published databases of TRE localization and noted that the mouse *Fgf21* locus harbors a TR-binding site in intron 2. This binding site was first detected in a study of TR-binding events near of T₃-target genes in cerebellum (Dong *et al.* 2009), which we later confirmed by our own genome wide assessment of TRβ1-binding events that utilized an engineered human HepG2 cell line that expresses exogenous TRβ1 (Ayers *et al.* 2014). We verified TR localization with human and mouse intron 2 using traditional ChIP-PCR approaches in HepG2 and native mouse liver and identified a functional TRE in this region of the mouse gene. We therefore suggest that TRs act through this intronic TRE to activate *FGF21* expression in HepG2 cells and that this effect is independent of PPARα signaling.

While our results indicate that TR can bind to a functional TRE in *FGF21* intron 2, we emphasize that they do not contradict the results of previous studies which indicate that TRs cooperate with PPARα to enhance *FGF21* proximal promoter activity (Adams *et al.* 2010). Unlike the *FGF21* proximal promoter, the putative *FGF21* intronic TRE does not respond to PPARα ligands. Furthermore, bezofibrate activation of the human *FGF21* gene is abolished by PPARα knockdown in HepG2 cells, with the T₃ response unaffected by PPARα knockdown. Thus, T₃ can activate the *FGF21* gene independently of PPARα. However, we also verified that TRβ and PPARα cooperate to elicit additive increases in *FGF21*-promoter-dependent luciferase reporter activity in transient transfections (results not shown). In the light of this study (Adams

et al. 2010) and other suggestions that TRs cooperate with PPARs to regulate gene expression (Lu & Cheng 2010), we suspect that TRs bound to the downstream intronic TRE can communicate with PPARα to regulate *FGF21* expression. This idea leads to the prediction that T₃ regulation of *FGF21* could be influenced by changes in PPARα activity and it will be interesting to see whether dietary conditions or administration of PPARα ligands could alter the patterns of hepatic T₃ regulation of *FGF21* or hepatic gene response in general.

As *FGF21* acts in an autocrine/paracrine fashion to regulate hepatic target genes involved in metabolic responses (Inagaki *et al.* 2007), we also tested the hypothesis that T₃-dependent regulation of hepatic gene expression programs would require *FGF21*. Specifically, we used an unbiased approach to determine whether responses to T₃ of any hepatic genes was diminished or abrogated in a mouse strain with a targeted deletion of the *Fgf21* gene locus. While T₃ regulates hundreds of genes in the livers of euthyroid mice, many with important roles in T₃-regulation of metabolic responses, there were limited differences in T₃ response patterns in WT and *Fgf21*^{-/-} mice. During our studies, a group led by Maratos-Flier *et al.* examined T₃

**Figure 7**

Analysis of serum metabolites in WT and *Fgf21*-knockout mice. (A) total serum cholesterol, (B) triglycerides, (C) glucose in WT and *Fgf21*^{-/-} mice after 3-day T₃ treatment. The statistical significance of the observed changes is denoted by double asterisks, which indicate *P* < 0.01.

regulation of metabolic parameters in *Fgf21*-knockout mice and the effects of administered FGF21 in hypothyroid and euthyroid mouse backgrounds (Domouzoglou *et al.* 2014). Results of this study revealed that T₃ and FGF21-dependent effects upon serum and hepatic lipid levels, thermogenesis and energy metabolism, and selected T₃ and FGF21 target genes are almost completely independent of the other hormone signaling system. Our transcriptome-wide gene expression studies extend and lend further support to this idea, and moreover, our own investigation of the effects of FGF21 and T₃ upon the levels of serum metabolites confirms that T₃-dependent reductions in total serum cholesterol are completely independent of FGF21.

We detected a small subset of hepatic genes that displayed diminished responses to T₃ in the *Fgf21*^{-/-} background. In principle, such genes could be indirect targets that lie downstream of the FGF21 peptide, or FGF21 could be a permissive factor for induction of direct TR targets, analogous to the hepatic PPAR α /FGF21 feed-forward loop established under fasting conditions in which FGF21 activation prolongs PPAR α -dependent responses (Badman *et al.* 2007, Inagaki *et al.* 2007). While we have not determined the mechanisms of these effects, we suspect that the latter mechanism is at play at least in regulation of *Dio1*, which contains bona fide TREs within its proximal promoter (Zhang *et al.* 1998). Perhaps more surprising, however, was that T₃/FGF21-dependent genes were associated with complement activation and the cell cycle and that many classical T₃-regulated genes involved in cholesterol metabolism (Lin *et al.* 2012, Lammell Lindemann *et al.* 2014), fatty acid synthesis, β -oxidation, and gluconeogenesis (Singh *et al.* 2013, Suh *et al.* 2013, Thakran *et al.* 2013) did not appear in this list. The significance of the dual T₃/FGF21 dependency displayed by this gene subset is not clear and requires further investigation.

We recognize that the notion that T₃ and FGF21 regulate hepatic metabolic response independently of each other must remain qualified for several reasons. We analyzed T₃-dependent changes in gene expression and serum lipid parameters after 72 h treatment. While this is long enough to obtain significant elevations of hepatic and serum FGF21 levels, it is possible that interactions between TR and FGF21-dependent pathways could emerge over longer treatment times. Furthermore, our studies were performed in euthyroid mice treated with T₃ and not hypothyroid mice. Thus, it is possible that some T₃- and FGF21-responsive genes with key roles in metabolic response could be fully induced at T₃ concentrations observed in euthyroid mice (data shown

in Lin *et al.* (2013)). Arguing against these possibilities, however, is the failure of the Maratos-Flier group also to identify defects in TR-dependent changes in metabolic parameters and gene expression in FGF21 knockouts over time courses of more than 1 week and in hypothyroid mice with varying levels of T₃ (Domouzoglou *et al.* 2014).

It also remains possible that some members of the T₃/FGF21-responsive gene subset could exert hard to predict effects upon metabolic responses. We attempted a more exhaustive effort to define the association of the T₃/FGF21-responsive gene subset with classical metabolic pathways and discovered possible association of genes with various aspects of lipid, amino acid, and carbohydrate metabolic pathways and insulin-dependent diabetes mellitus (Table 4). For example, *DIO1* encodes a product that catalyzes the conversion of T₄ to T₃ and therefore will alter local TH levels and, potentially, TR actions upon key genes involved in cholesterol metabolism. *INSIG2* is an inhibitor of sterol response element-binding protein (SREBP) activation and changes in levels of this transcription factor could result in widespread secondary alterations in the expression patterns of genes that regulate lipid metabolism. While it is conceivable that altered cooperation of TH and FGF21 at these, and other, genes could ultimately result in changes in systemic cholesterol and lipid levels, such effects were not obvious over the course of our study (Fig. 7). At present our results are most consistent with the notion that T₃-dependent hepatic gene regulation patterns are largely independent of FGF21 signaling.

Declaration of interest

The authors declare that there is no conflict of interest that could be perceived as prejudicing the impartiality of the research reported.

Funding

This study was supported by NIH RC4 DK090849 (P W) and National Natural Science Foundation of China No. 81270868 (X X).

Author contribution statement

XX and P W designed the experiments; A Z, J P Y, J H S and S D A performed the research; G E W, D H S, A K, C P and P Z contributed reagents/analytical tools and; analyzed data; and X X and P W wrote the paper.

Acknowledgements

The authors wish to honor the memory of John D Baxter (deceased) whose insights into thyroid hormone inspired this study. They thank Dr Steven A Klierer who provided us the FGF21-knockout mice for this study.

References

- Adams AC, Astapova I, Fisher FM, Badman MK, Kurgansky KE, Flier JS, Hollenberg AN & Maratos-Flier E 2010 Thyroid hormone regulates hepatic expression of fibroblast growth factor 21 in a PPAR α -dependent manner. *Journal of Biological Chemistry* **285** 14078–14082. (doi:10.1074/jbc.C110.107375)
- Ayers S, Switnicki MP, Angajala A, Lammel J, Arumanayagam AS & Webb P 2014 Genome-wide binding patterns of thyroid hormone receptor β . *PLoS ONE* **9** e81186. (doi:10.1371/journal.pone.0081186)
- Badman MK, Pissios P, Kennedy AR, Koukos G, Flier JS & Maratos-Flier E 2007 Hepatic fibroblast growth factor 21 is regulated by PPAR α and is a key mediator of hepatic lipid metabolism in ketotic states. *Cell Metabolism* **5** 426–437. (doi:10.1016/j.cmet.2007.05.002)
- Baxter JD & Webb P 2009 Thyroid hormone mimetics: potential applications in atherosclerosis, obesity and type 2 diabetes. *Nature Reviews. Drug Discovery* **8** 308–320. (doi:10.1038/nrd2830)
- Benjamini Y & Hochberg Y 1995 Controlling the false discovery rate: a practical and powerful approach to multiple testing. *Journal of the Royal Statistical Society. Series B (Methodological)* **57** 289–300. (doi:10.2307/2346101)
- Berglund ED, Li CY, Bina HA, Lynes SE, Michael MD, Shanafelt AB, Kharitonov A & Wasserman DH 2009 Fibroblast growth factor 21 controls glycemia via regulation of hepatic glucose flux and insulin sensitivity. *Endocrinology* **150** 4084–4093. (doi:10.1210/en.2009-0221)
- Chatonnet F, Guyot R, Benoit G & Flamant F 2013 Genome-wide analysis of thyroid hormone receptors shared and specific functions in neural cells. *PNAS* **110** E766–E775. (doi:10.1073/pnas.1210626110)
- Cheng SY, Leonard JL & Davis PJ 2010 Molecular aspects of thyroid hormone actions. *Endocrine Reviews* **31** 139–170. (doi:10.1210/er.2009-0007)
- Coskun T, Bina HA, Schneider MA, Dunbar JD, Hu CC, Chen Y, Moller DE & Kharitonov A 2008 Fibroblast growth factor 21 corrects obesity in mice. *Endocrinology* **149** 6018–6027. (doi:10.1210/en.2008-0816)
- Domouzoglou EM & Maratos-Flier E 2011 Fibroblast growth factor 21 is a metabolic regulator that plays a role in the adaptation to ketosis. *American Journal of Clinical Nutrition* **93** 901S–905S. (doi:10.3945/ajcn.110.001941)
- Domouzoglou EM, Fisher FM, Astapova I, Fox EC, Kharitonov A, Flier JS, Hollenberg AN & Maratos-Flier E 2014 Fibroblast growth factor 21 and thyroid hormone show mutual regulatory dependency but have independent actions *in vivo*. *Endocrinology* **155** 2031–2040. (doi:10.1210/en.2013-1902)
- Dong H, Yauk CL, Rowan-Carroll A, You SH, Zoeller RT, Lambert I & Wade MG 2009 Identification of thyroid hormone receptor binding sites and target genes using ChIP-on-chip in developing mouse cerebellum. *PLoS ONE* **4** e4610. (doi:10.1371/journal.pone.0004610)
- Du P, Kibbe WA & Lin SM 2008 lumi: a pipeline for processing Illumina microarray. *Bioinformatics* **24** 1547–1548. (doi:10.1093/bioinformatics/btn224)
- Dutchak PA, Katafuchi T, Bookout AL, Choi JH, Yu RT, Mangelsdorf DJ & Kliewer SA 2012 Fibroblast growth factor-21 regulates PPAR γ activity and the antidiabetic actions of thiazolidinediones. *Cell* **148** 556–567. (doi:10.1016/j.cell.2011.11.062)
- Fon Tacer K, Bookout AL, Ding X, Kurosu H, John GB, Wang L, Goetz R, Mohammadi M, Kuro-o M, Mangelsdorf DJ *et al.* 2010 Research resource: comprehensive expression atlas of the fibroblast growth factor system in adult mouse. *Molecular Endocrinology* **24** 2050–2064. (doi:10.1210/me.2010-0142)
- Gagne R, Green JR, Dong H, Wade MG & Yauk CL 2013 Identification of thyroid hormone receptor binding sites in developing mouse cerebellum. *BMC Genomics* **14** 341. (doi:10.1186/1471-2164-14-341)
- Iglesias P, Selgas R, Romero S & Diez JJ 2012 Biological role, clinical significance, and therapeutic possibilities of the recently discovered metabolic hormone fibroblastic growth factor 21. *European Journal of Endocrinology* **167** 301–309. (doi:10.1530/EJE-12-0357)
- Inagaki T, Dutchak P, Zhao G, Ding X, Gautron L, Parameswara V, Li Y, Goetz R, Mohammadi M, Esser V *et al.* 2007 Endocrine regulation of the fasting response by PPAR α -mediated induction of fibroblast growth factor 21. *Cell Metabolism* **5** 415–425. (doi:10.1016/j.cmet.2007.05.003)
- Johnson CL, Weston JY, Chadi SA, Fazio EN, Huff MW, Kharitonov A, Koester A & Pin CL 2009 Fibroblast growth factor 21 reduces the severity of cerulein-induced pancreatitis in mice. *Gastroenterology* **137** 1795–1804. (doi:10.1053/j.gastro.2009.07.064)
- Kliewer SA & Mangelsdorf DJ 2010 Fibroblast growth factor 21: from pharmacology to physiology. *American Journal of Clinical Nutrition* **91** 254S–257S. (doi:10.3945/ajcn.2009.28449B)
- Lammel Lindemann JA, Angajala A, Engler DA, Webb P & Ayers SD 2014 Thyroid hormone induction of human cholesterol 7 α -hydroxylase (Cyp7a1) *in vitro*. *Molecular and Cellular Endocrinology* **388** 32–40. (doi:10.1016/j.mce.2014.02.003)
- Lin JZ, Martagon AJ, Hsueh WA, Baxter JD, Gustafsson JA, Webb P & Phillips KJ 2012 Thyroid hormone receptor agonists reduce serum cholesterol independent of the LDL receptor. *Endocrinology* **153** 6136–6144. (doi:10.1210/en.2011-2081)
- Lin JZ, Sieglaff DH, Yuan C, Su J, Arumanayagam AS, Firouzbakht S, Cantu Pompa JJ, Reynolds FD, Zhou X, Cvorova A *et al.* 2013 Gene specific actions of thyroid hormone receptor subtypes. *PLoS ONE* **8** e52407. (doi:10.1371/journal.pone.0052407)
- Lu C & Cheng SY 2010 Thyroid hormone receptors regulate adipogenesis and carcinogenesis via crosstalk signaling with peroxisome proliferator-activated receptors. *Journal of Molecular Endocrinology* **44** 143–154. (doi:10.1677/JME-09-0107)
- Paquette MA, Dong H, Gagne R, Williams A, Malowany M, Wade MG & Yauk CL 2011 Thyroid hormone-regulated gene expression in juvenile mouse liver: identification of thyroid response elements using microarray profiling and *in silico* analyses. *BMC Genomics* **12** 634. (doi:10.1186/1471-2164-12-634)
- Ramadoss P, Abraham BJ, Tsai L, Zhou Y, Costa-e-Sousa RH, Ye F, Bilban M, Zhao K & Hollenberg AN 2014 Novel mechanism of positive versus negative regulation by thyroid hormone receptor β 1 (TR β 1) identified by genome-wide profiling of binding sites in mouse liver. *Journal of Biological Chemistry* **289** 1313–1328. (doi:10.1074/jbc.M113.521450)
- R Development Core Team 2010 R: A language and environment for statistical computing. R Foundation for Statistical Computing, Vienna, Austria. ISBN 3-900051-07-0, URL <http://www.R-project.org/>.
- Singh BK, Sinha RA, Zhou J, Xie SY, You SH, Gauthier K & Yen PM 2013 FoxO1 deacetylation regulates thyroid hormone-induced transcription of key hepatic gluconeogenic genes. *Journal of Biological Chemistry* **288** 30365–30372. (doi:10.1074/jbc.M113.504845)
- Smyth GK 2005 Limma: linear models for microarray data. In *Bioinformatics and Computational Biology Solutions using R and Bioconductor*, pp 397–420. Eds R Gentleman, V Carey, S Dudoit, R Irizarry & W Huber. New York: Springer.
- Suh JH, Sieglaff DH, Zhang A, Xia X, Cvorova A, Winnier GE & Webb P 2013 SIRT1 is a direct coactivator of thyroid hormone receptor β 1 with gene-specific actions. *PLoS ONE* **8** e70097. (doi:10.1371/journal.pone.0070097)
- Tabas-Madrid D, Nogales-Cadenas R & Pascual-Montano A 2012 GeneCodis3: a non-redundant and modular enrichment analysis tool for functional genomics. *Nucleic Acids Research* **40** W478–W483. (doi:10.1093/nar/gks402)
- Thakran S, Sharma P, Attia RR, Hori RT, Deng X, Elam MB & Park EA 2013 Role of sirtuin 1 in the regulation of hepatic gene expression by thyroid hormone. *Journal of Biological Chemistry* **288** 807–818. (doi:10.1074/jbc.M112.437970)
- Wei W, Dutchak PA, Wang X, Ding X, Wang X, Bookout AL, Goetz R, Mohammadi M, Gerard RD, Dechow PC *et al.* 2012 Fibroblast growth

- factor 21 promotes bone loss by potentiating the effects of peroxisome proliferator-activated receptor γ . *PNAS* **109** 3143–3148. (doi:10.1073/pnas.1200797109)
- Xu J, Lloyd DJ, Hale C, Stanislaus S, Chen M, Sivits G, Vonderfecht S, Hecht R, Li YS, Lindberg RA *et al.* 2009 Fibroblast growth factor 21 reverses hepatic steatosis, increases energy expenditure, and improves insulin sensitivity in diet-induced obese mice. *Diabetes* **58** 250–259. (doi:10.2337/db08-0392)
- Yuan C, Lin JZ, Sieglaff DH, Ayers SD, Denoto-Reynolds F, Baxter JD & Webb P 2012 Identical gene regulation patterns of T₃ and selective thyroid hormone receptor modulator GC-1. *Endocrinology* **153** 501–511. (doi:10.1210/en.2011-1325)
- Zhang CY, Kim S, Harney JW & Larsen PR 1998 Further characterization of thyroid hormone response elements in the human type 1 iodothyronine deiodinase gene. *Endocrinology* **139** 1156–1163. (doi:10.1210/endo.139.3.5849)

Received in final form 8 December 2014

Accepted 11 December 2014

Accepted Preprint published online 11 December 2014